An Acad Bras Cienc (2024) 96(Suppl. 1): e20231051 DOI 10.1590/0001-3765202420231051
Anais da Academia Brasileira de Ciências | *Annals of the Brazilian Academy of Sciences*
Printed ISSN 0001-3765 I Online ISSN 1678-2690
www.scielo.br/aabc | www.fb.com/aabcjournal

GEOSCIENCES

Explosive cyclones occurred between 2010 and 2020 in the South Atlantic under the perspective of two detection schemes

HUGO N. ANDRADE, MÁRIO FRANCISCO L. DE QUADRO, ANDRÉ B. NUNES, FABRÍCIO S.C. DE OLIVEIRA, VILSON D. DE AVILA, MATEUS S. TEIXEIRA, & RITA DE CÁSSIA M. ALVES

Abstract: Under two detection schemes, this study analyzes one of the most destructive weather systems - the explosive cyclones - in the South Atlantic, from 2010 to 2020. Then, two methods are presented to study these systems: the Observational Method (OBSM) and the Automated Method (AUTM). The first uses visual analysis of the mean sea level pressure (mslp) fields and functions to identify the local minimums using the Grid Analysis and Display (GrADS) software. The second utilizes a function from OpenGrADS called *mfhilo*. It shows the local minimum in the grid using laplacian, magnitude, and percentile. Two shell algorithms for data manipulation are used for the AUTM: one to trace the cyclones' trajectories according to a previously defined fixed area and the other to separate them into explosives. The OBSM methodology showed 271 cases averaging 25 yearly and revealed important characteristics regarding the intensities. According to AUTM's methodology, from the 2705 ordinary cyclone cases identified, 299 are explosives. There is a clear seasonality pattern in the systems' distribution along South America, similar to OBSM, but more highlighted. In summer, they concentrate at high latitudes, while in winter and spring, they are assembled near southern Brazilian and Uruguayan coasts.

Key words: Climatology Tool, Computational Algorithm, Cyclogenesis, Cyclone Detection, Automated Method, Manual Method.

INTRODUCTION

The abundant rain that sustains life on Earth is not just compensation for cloud microphysics processes. Without continuous and vigorous movements, the atmospheric part of the hydrological cycle would stagnate (Wallace & Hobbs 2006). Such movements are closely linked to weather systems with well-defined structures.

Specifically, in the south-central region of South America, weather and climate are strongly influenced by various types of systems such as fronts, cyclones, squall lines, and mesoscale systems (Satyamurty et al. 1998, Avila et al. 2021). Among those mentioned, extratropical cyclones and their associated fronts are the meteorological systems that most reach the area because they are located at mid and high latitudes. Cyclone formation, determined as cyclogenesis, and its development in the atmosphere have been studied since the 19th century due to its essential role in transporting heat, humidity, and momentum (Palmén & Newton 1969, Peixoto & Oort 1992, Gan & Seluchi 2009). On the other hand, cyclones are linked to strong winds, floods, heavy rains, and dangerous oceanic

conditions, resulting in socioeconomic losses, especially in coastal cities (Allen et al. 2010, Reboita et al. 2010, Liberato et al. 2011, Neu et al. 2013, Reale & Lionello 2013, Reale et al. 2019).

The rapid intensification of extratropical cyclones has been a research subject in recent decades due to the damage they caused and the failure of operational models to predict this type of phenomenon. Tor Bergeron studied explosive cyclones, but the adaptations of Sanders & Gyakum (1980) brought more significant contributions. Called bombs, they are defined as negative relative vorticity systems in the Southern Hemisphere, where the central pressure drops at an average rate of at least 1 Bergeron (Eq. 1). When corrected by latitude, this rate, defined to 60º, can range from 13,9 hPa/24 hours at 30° to 27,7 hPa/24 hours at the poles (Wang & Rogers 2001). Bombs are predominantly marine, occur preferably in winter, and often present hurricane characteristics in wind and cloud fields (Sanders & Gyakum 1980).

There is a significant disparity in the amount of research on explosive cyclones between the North and the South Atlantic. While the former has been the subject of numerous studies, only a few have focused explicitly on the latter. In recent years, several systems have hit Brazil, Uruguay, and Argentina's coastal regions and caused lots of damage. Consequently, it is vital to provide society with an accurate diagnosis of cyclonic activity, frequency, movement, and possible changes (Neu et al. 2013, Reboita et al. 2021). With this in mind, we need pressure systems detection schemes that can provide important information, applied with increasingly robust data. These investigations can influence decision-makers in creating public policies to mitigate the effects of weather systems, especially in more vulnerable areas.

These algorithms have more coverage for tropical cyclones due to the damage caused, especially in the North Atlantic, and because they have a more regular structure (Wang et al. 2020, Prantl et al. 2021). However, extratropical cyclones, especially explosives, are no less relevant. Identifying the displacement of extratropical cyclones seems to be a simple task, but it presents difficulties. Since its occurrence is common, confusing it with other systems may be usual. In addition, they can vary in size, structure (asymmetric), and speed. Also, another characteristic that hinders identification is the diversity in synoptic situations (Neu et al. 2013), which results in different detection schemes.

Observational methods are very reliable because they employ the user experience as a guide to the systems' behavior during their trajectory. However, they are very costly concerning working time, and the day-to-day analysis can also negatively affect long-term studies (Prantl et al. 2021). In the 90s, these difficulties led to the first automated cyclone detection schemes. One of the most outstanding was developed by Murray & Simmonds (1991), designed for the Southern Hemisphere using surface pressure. Then came other methods based on pressure and vorticity at the surface and low levels (Sinclair 1995, 1997, Hoskins & Hodges 2005, Rudeva & Gulev 2007, Hanley & Caballero 2012, Flaounas et al. 2014, Lu 2017, Prantl et al. 2021).

The main reason to use automated methods is to get a tool fed with multiple data sources. This makes it possible to analyze essential parameters, such as distribution, frequency, and evolution, as well as observe changes over time, especially with climate change (Lu 2017, Prantl et al. 2021). In large part, the known algorithms analyze extratropical cyclones in general, not discriminating them into explosives, which results in the generalization of systems. Thus, this work aims to study the cases of explosive cyclones in the South Atlantic from 2010 to 2020 under the perspective of two detection schemes: manual and automated.

MATERIALS AND METHODS

Data

Data from ERA5 reanalysis were used, with a spatial resolution of 0,25° x 0,25°, hourly temporal resolution, and 37 vertical levels available at the platform (Hersbach et al. 2020). The data were selected between January 2010 and December 2020, with a 3-hour interval. ERA5 reanalysis is the fifth generation, benefiting from ten years of improvements over the previous product, ERA-Interim (Dee et al. 2011), mainly in the model physics, dynamics, and data assimilation, in addition to the more refined spatial resolution (Hersbach et al. 2020). The product uses the best observational and satellite data, utilizing the Integrated Forecast System (IFS) Cy41r2.

The other reanalysis data used were from the Climate Forecast System Reanalysis (CFSR) and the Climate Forecast System version 2 (CFSv2), made available by the National Center for Environmental Prediction (NCEP). Both have a 0,5° x 0,5° spatial resolution with a 6-hour temporal resolution, covering the synoptic times (00Z, 06Z, 12Z, 18Z) and a vertical grid ranging from 1000 hPa to 1 hPa with 37 vertical levels. The first set has data available from January 1979 to March 2011 (Saha et al. 2006), and the second from April 2011 to the present (Saha et al. 2014). This product was developed to simulate the domain conditions of the coupled system atmosphere-ocean-land-sea ice. This reanalysis covers the same period of ERA5, except for the difference in temporal resolution.

Observational Method (OBSM)

Regarding the observational method (OBSM) for case detection, the regions with trough and closed isobars in the mean sea level pressure (mslp) field were initially visually identified. The procedure was made within the spatial domain (15°S and 60°S, 75°W and 10°W) for the entire study period with ERA5 reanalysis through the Grid Analysis and Display (GrADS) software (Doty & Kinter III 1995) version 2.2.1.

In the second stage, a visual variable domain was determined according to the situation of the mslp field in the regions previously identified, which included the troughs and closed isobars. The mslp minimum (i.e., grid point value lower than its neighbor points - local minimum) was returned through the *amin* function from GrADS software within this cited domain. Converting to latitude and longitude (*aminlocy* and *aminlocx* commands, respectively) was necessary to obtain the exact location. It is emphasized that the *amin* function sweeps a specific grid on lines from south to north and each line from west to east, strictly in this order. Fig. 1 exemplifies this process, in which the dotted black frames show the grid used by the amin, aminlocy, and aminlocx functions.

After tracking the cyclone's development, from its cyclogenesis to the most intense phase, the Normalized Deepening Rate (NDR) is calculated, defined by Sanders & Gyakum (1980):

ΔPc is the change of the central pressure in 24 hours [mslp(t) - mslp(t+24h)] and φ is the average latitude, considering the beginning and end points of the explosive phase (red dotted lines indicating initial and final latitudes - Fig. 1). When this rate equals or exceeds 1 Bergeron (B), the cyclone is considered a "bomb" or explosive.

Explosive cyclones were differentiated in intensity using the following criteria: i) $1.00 \leq NDR < 1.30$ are weak; ii) $1.30 \leq NDR \leq 1.80$ are moderate; iii) $NDR > 1.80$ are intense. This classification differs minimally from the one proposed by Sanders (1986), which discriminates weak explosive cyclones as

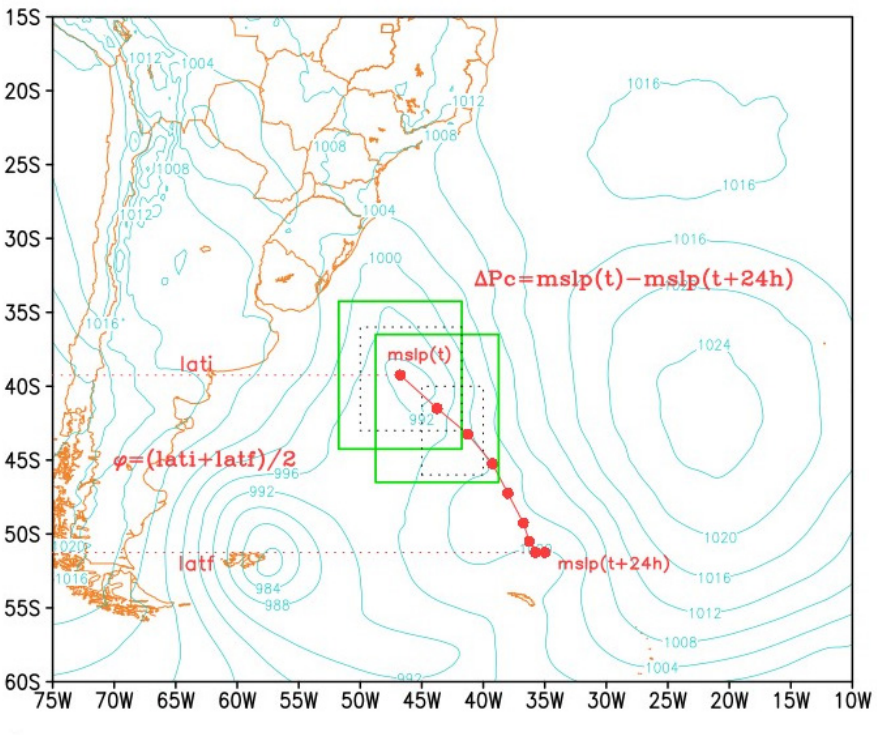

Figure 1. South American area where the cases were submitted to the detection scheme. The red dots denote the cyclone's trajectory example in the explosive phase. The dotted black frames demonstrate the variable domain covering the cyclone for minimum mslp detection. In green, the area where the following mslp minimum must be identified. The blue mslp field refers to the same timestep of the first minimum identified (03Z01032014).

1.0 ≤ NDR ≤ 1.2 and moderates as 1.3 ≤ NDR ≤ 1.8. Since this study utilizes two decimal places, weak and moderate are minimally altered (Andrade et al. 2022).

It is highlighted that an mslp minimum identified in a given timestep that moved more than 5º of latitude or longitude related to a previous timestep (represented by the light green squares - Fig. 1) was considered as if there was a formation of a new low pressure or discarded because it did not reach this displacement condition.

This characteristic coincides with that applied by Zhang et al. (2017), who used 6-hour intervals and, during the visual inspection, defined a 10° latitude x 16° longitude box. Since this study uses 3-hour intervals, the choice of latitude and longitude detection threshold is justified.

At high latitudes, it is common for a cyclone to start near another preexisting one (Fedorova 2001, Wang & Rogers 2001). Therefore, the applied criterion helps to filter these conditions along with visual analysis.

These visually identified cases were confronted with the synoptic charts distributed by the Center for Weather Forecasting and Climate Studies (CPTEC), identifying the low pressures and their respective cold and warm fronts. These charts come from the GFS model and can be accessed in the institution's repository via the link: http://img0.cptec.inpe.br/~rgptimg/Produtos-Pagina/Carta-Sinotica/Analise/Superficie.

It is important to emphasize that the method is semi-automated because the GrADS commands perform the mslp minimum detection, but it is highly dependent on visual analysis. Therefore, it was preferred to use the nomenclature observational method.

Automated Method (AUTM)

After analyzing the cases through OBSM methodology, an automated cyclone detection method was developed using CFSR, CFSv2, and ERA5 reanalysis. Figs. 2, 3, and 4 show the organizational chart illustrating the algorithm.

In summary, Fig. 2 illustrates the part of the algorithm that selects the mslp minimums. It writes these values and coordinates in annual output files and plots mslp fields with the minimum detected. Fig. 3 presents the routine that defines cyclones' trajectories in the domain established in Fig. 1, considering the pre-established parameters such as the coverage area and the maximum period of displacement. Fig. 4 shows the final part of the algorithm that selects cyclones over 24 hours and classifies them into explosive or non-explosive. Finally, sensitivity tests were performed to define which parameters best fit the classification of explosive cyclones defined by AUTM compared to those found by OBSM.

As an initial part, a namelist is used as an application input to determine some variables that will be utilized in simulating the cyclone detection computational algorithm.

A function called *mfhilo* (Fig. 2), from the Open Grid Analysis and Display (OpenGrADS) software version 2.2.1.oga.1, was used to achieve the objective of cyclone identification. OpenGrADS is an open project for developing interfaces and applications based on GrADS mechanisms. This function finds the minimum values of the variable in a spatial dimension field, varying latitude (lat) and longitude (lon). Therefore, the location and the selected minimum locations in the delimited region are returned. In this function, the Grid-Based (GR) method was ordered by laplacian, magnitude, and a predefined percentile (indicates the number of points that will be shown). At the same time, the

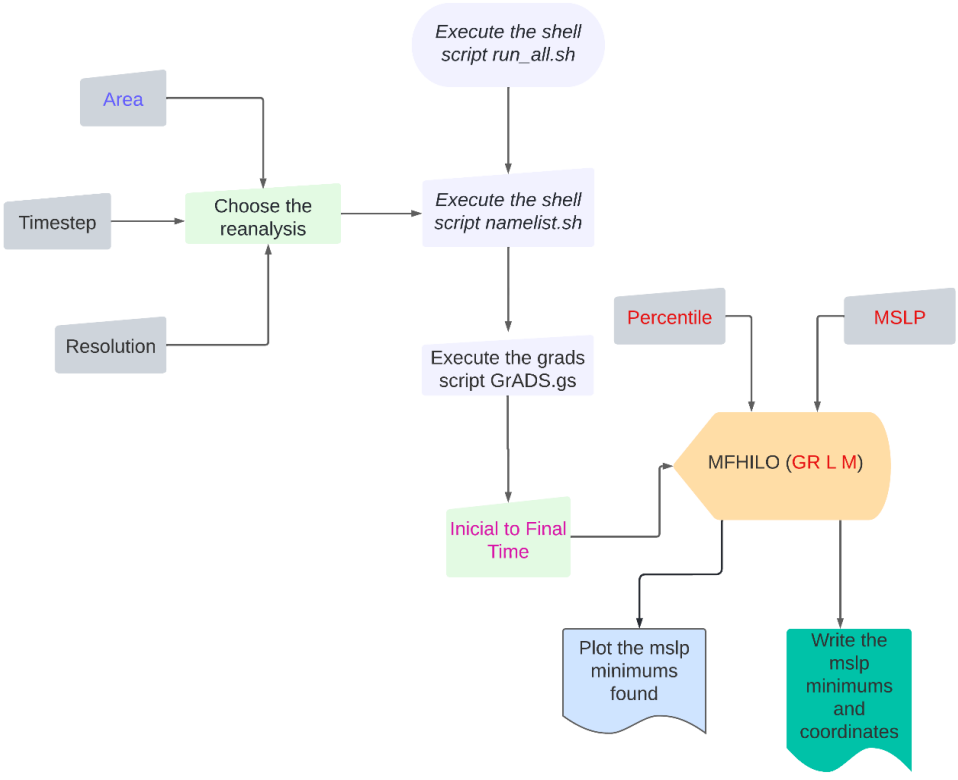

Figure 2. An organizational chart describing the detection steps for mslp minimum through the "*mfhilo*" function in AUTM.

local minimums are identified, and all of them are stored in a single annual matrix text file next to the respective dates, latitudes, and longitudes. Also, the mslp fields are plotted, enabling the user to verify the density of minimums and their correspondence with the low pressures.

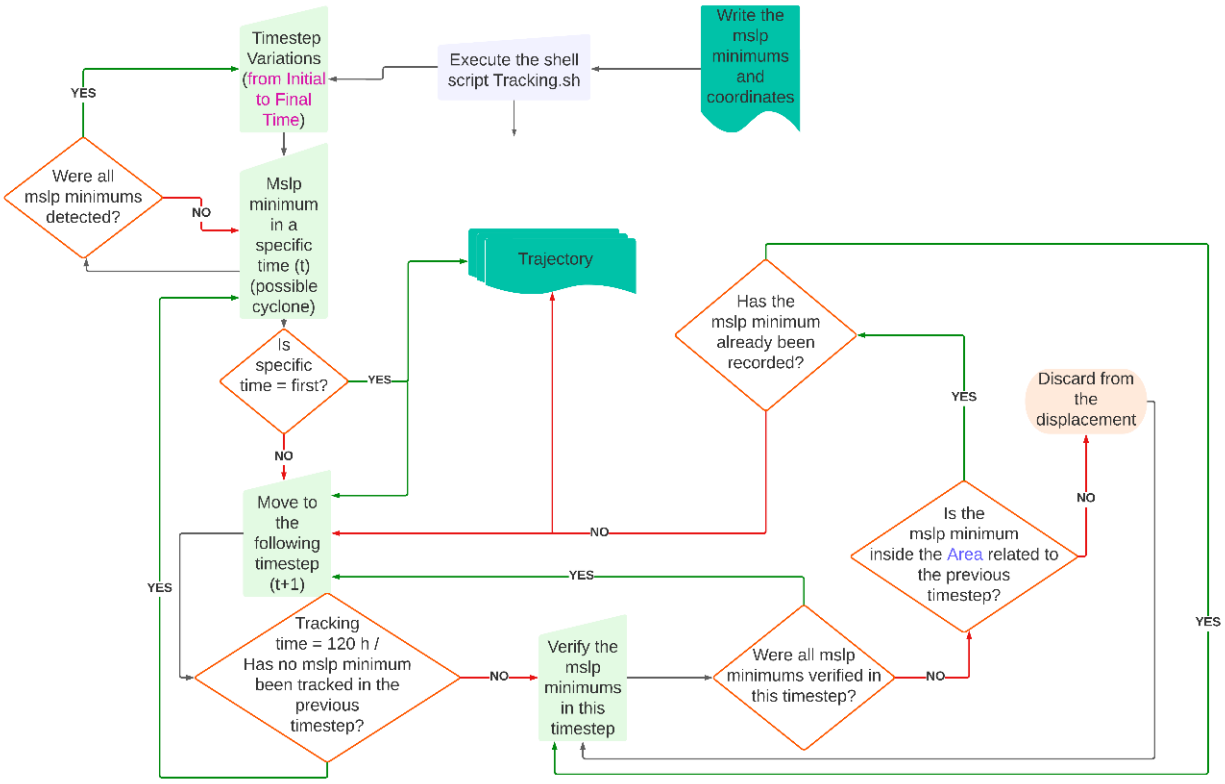

Figure 3. An organizational chart representing the algorithm part that develops a possible cyclone's trajectory.

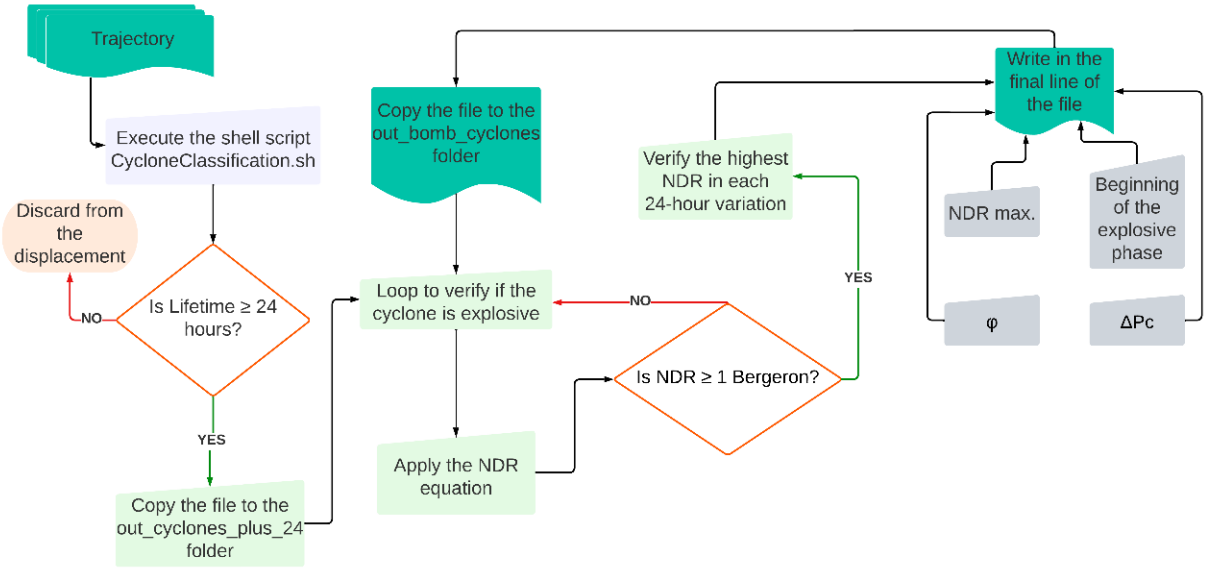

Figure 4. An organizational chart classifying cyclones into greater than or equal to 24 hours and explosives.

Once the mslp minimums are found, the next part of AUTM is dedicated to the trajectory of a possible cyclone in a specific time (t), shown in Fig. 3. After a simple check, if this timestep is the first one of the tracking, the algorithm moves on to the next timestep. In the sequence, there is a scan on all other mslp minimums detected in the following timestep (t+1). It is checked if any mslp minimum point is inside the fixed area (input in the namelist - Fig. 2) concerning the previous point. If this criterion is met, the value is stored in the same text file as the last point. If not, it is discarded from the trajectory.

This tracking can continue until the algorithm satisfies any of the following conditions: i) find no more mslp minimum inside the area; ii) reach the domain limits (no data); iii) if the tracking lasts 120 hours (5 days). Once one criterion is met, it returns to (t), and another mslp minimum of that timestep enters the abovementioned process. If in (t), there are no more mslp minimum values, the posterior timestep becomes (t) to cover the entire period under study (from 2010 to 2020).

It is important to note that the trajectory storage in a text file is done with the first minimum found inside the area - the same characteristic applied by the OBSM. This restriction was applied to prevent more than one mslp minimum value described in the trajectory for a given timestep, especially at higher resolutions.

Once the tracking is determined for the entire period, there can be files with only one synoptic time or up to 120 hours (5 days). Next, cyclones pass through filters in this part of AUTM (Fig. 4). The first condition is that the cyclone has a lifetime greater than or equal to 24 hours. Once these are separated, the second condition is to calculate the NDR (Eq. 1) for each 24-hour variation within the files. If in a given period (e.g., from 00ZdayX to 00ZdayX+1), the NDR equals or exceeds 1 B, and there is no higher value for the variable, this will be marked as the explosive phase of the cyclone (NDR max). The NDR can occur in cyclogenesis (explosive cyclogenesis) or during cyclone development.

The resulting template of each organizational chart was repeated at the beginning of the following. In such a manner, it facilitates understanding, and the sequence of events is guaranteed since the information generated is necessary for the next step.

It is well known that some algorithms use vorticity to detect cyclones as it is proportional to the Laplacian of the geopotential height or pressure fields and may detect the system in earlier stages. However, as a disadvantage arising from this variable, many “false positives” can occur, reflecting small-scale variations in a geopotential height or pressure field that are not early-stage cyclones as understood by synoptic analysts (Roebber et al. 2023). These small-scale variations were noticed in initial tests using vorticity in the main lower levels of the atmosphere and did not actually present the cyclone previously observed in the OBSM. To avoid using additional forms of smoothing or filtering and to better compare the results with OBSM, our methodology presented better results using mslp fields to identify the cyclones.

After completing the algorithm, sensitivity tests were performed to determine the percentile and area values best adapted to the reanalysis. The year 2014 was chosen because it was the bombs’ highest absolute frequency by the OBSM method. The tests were made varying 75, 85, and 95 percentiles and 3-, 5-, 7-, and 9-degree areas, totaling 12 tests. The validation was performed by comparing the explosive cyclone cases found, varying these parameters, with the cases caught by OBSM. Finally, a last test was executed to compare the results of the CFSR/CFSv2 and ERA5 reanalysis, where the difference between them was considered since they present different spatial resolutions.

RESULTS AND DISCUSSIONS

Observational Method (OBSM)

The most direct method for acquiring tracking is through the process of manual observation (Sander & Gyakum 1980, Roebber 1984, Gyakum et al. 1989, Avila et al. 2021, Andrade et al. 2022, Roebber et al. 2023). One significant advantage of this method is that the users can sift through these data, allowing them to notice peculiarities, such as a secondary development, which would otherwise be missed. In addition, the analysts' synoptical knowledge benefits from this method (Roebber et al. 2023).

The analysis of explosive cyclone cases in the South Atlantic by the observational method showed that, through ERA5 data, 271 cases were identified from 2010 to 2020. There was an average of approximately 25 cases per year, with the maximum in 2014 (29) and the minimum in 2017 (20). Lim & Simmonds (2002), in climatology for the Southern Hemisphere, found similar values for the whole region, through NCEP2 reanalysis (2,5º x 2,5º spatial resolution), with an average of 26 cases per year. Reale et al. (2019) emphasize that cyclones near South America have higher Normalized Deepening Rates and duration than those near Australia. This may also have impacted the difference for the study by Lim & Simmonds (2002).

In the seasonal distribution, it was seen that the higher frequency was observed in winter, then autumn, followed by spring and summer with the same number. This survey agrees with previous climatologies (Lim & Simmonds 2002, Mendes et al. 2010, Allen et al. 2010, Bitencourt et al. 2013). In addition, Table I attests to the highest frequency of cases in June (31) and the smallest in April (18). Besides, there is a significant increase from 2018 to 2020 during June, representing the highest frequency in the sample.

It was found that the intensity of explosive cyclones does not follow a normal distribution, which was expected, since ordinary cyclones present higher frequency than explosive ones (Fig. 5). The illustration shows the intensities' histogram with asymmetrical distribution to the right and mode

Table I. Explosives cyclones' monthly frequency during the analyzed period.

	2010	2011	2012	2013	2014	2015	2016	2017	2018	2019	2020	TOTAL
January	4	1	0	0	2	3	4	2	3	3	1	**23**
February	4	1	2	1	3	1	4	0	0	1	1	**18**
March	1	4	2	1	4	1	0	2	2	1	1	**19**
April	0	1	2	3	1	1	3	2	1	1	2	**17**
May	2	1	3	3	2	3	4	0	4	2	1	**25**
June	4	3	2	2	3	2	0	1	4	5	5	**31**
July	3	1	5	3	0	3	4	1	3	3	4	**30**
August	2	5	2	3	4	1	0	3	1	1	4	**26**
September	2	2	1	1	2	5	1	2	2	1	1	**20**
October	3	2	2	2	3	2	2	4	1	1	2	**24**
November	0	0	3	1	2	1	4	2	3	1	1	**18**
December	1	1	4	3	3	1	1	1	0	3	2	**20**
TOTAL	**26**	**22**	**28**	**23**	**29**	**24**	**27**	**20**	**24**	**23**	**25**	**271**

between the (1.10;1.20] interval. Regarding the frequencies, since 3 cases presented the exact 1.30 value, 127 weak, 104 moderate, and 40 intense were detected.

The boxplot in Fig. 6 demonstrates the monthly intensity distribution. The distance between the upper (third quartile) and lower (first quartile) limits shows the high amplitude of intensities during all months, while the distance between the median line and mean (X) indicates an asymmetry of data in most months. Concerning the mean, the line connecting the different boxes indicates a smooth oscillation pattern between months. After the minimum, there is a peak in the next month and a subsequent decrease in this mean in the following two. This indicates that every two months, there is

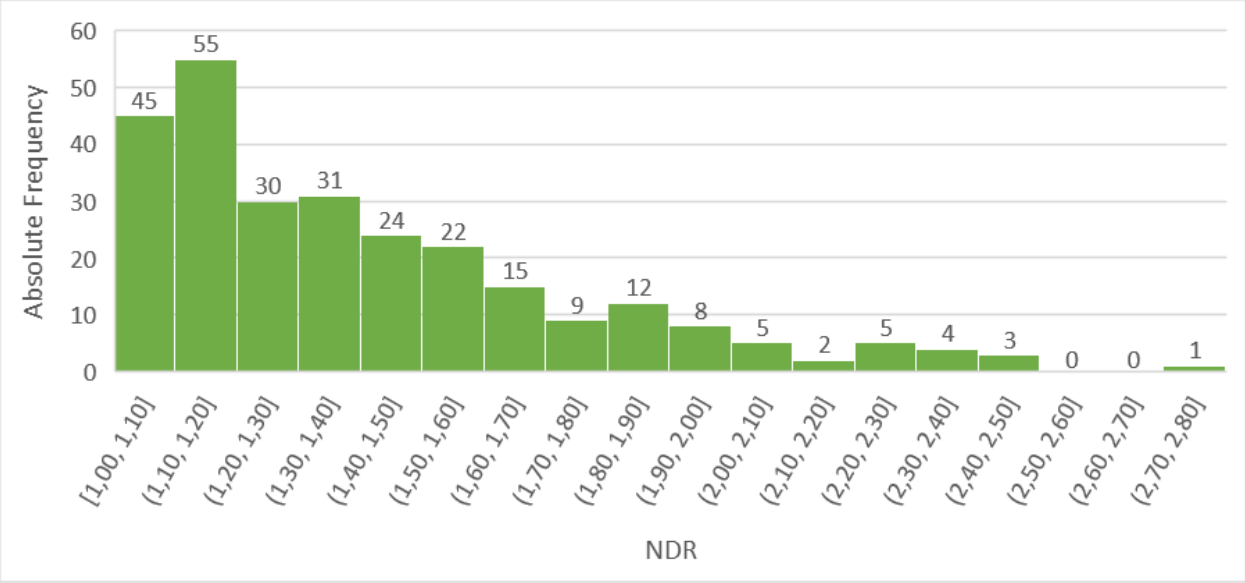

Figure 5. Explosive cyclones intensities histogram.

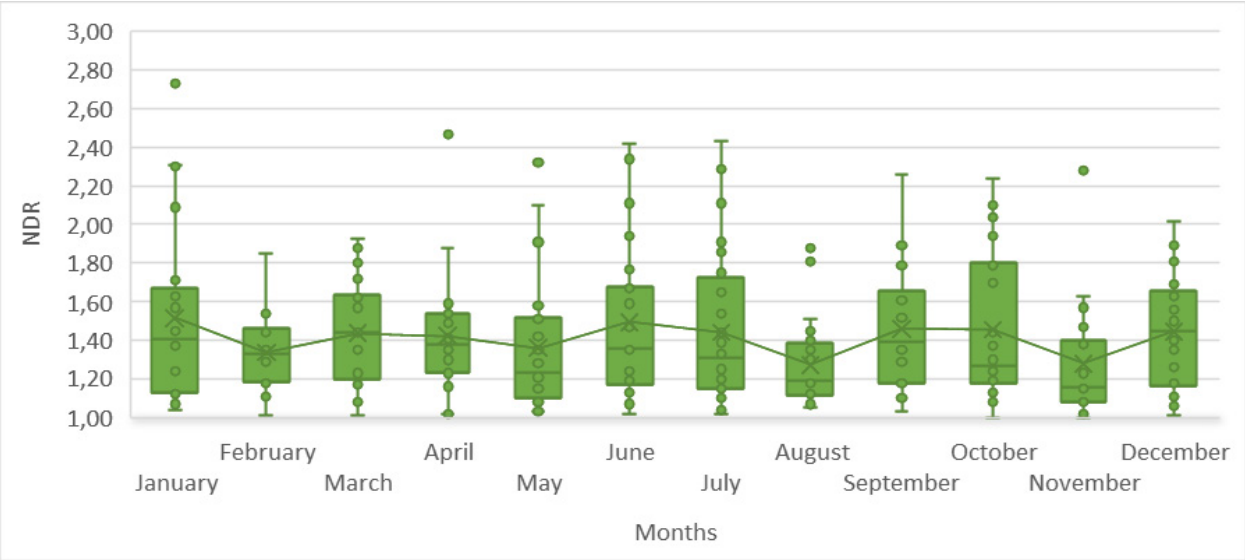

Figure 6. Boxplot showing the monthly distribution according to the Normalized Deepening Rate. Cases with the respective intensities are marked as green circles. Each box has a lower and upper limit (first and third quartiles), a horizontal line (median), and an X denoting the mean. A line interconnects the means.

an increase in the mean intensity of explosive cyclone cases in the South Atlantic. A higher frequency of intense cases was observed in July and October.

Fig. 7 exhibits the trajectories of weak (green), moderate (yellow), and intense (red) explosive cyclones by OBSM according to the seasons (summer (a); autumn (b); winter (c); and spring (d)). The figures show the starting point of each cyclone up to the end of the explosive phase. We can observe some cases with only a closed circular point, which indicates that cyclogenesis has already begun explosively. The open circular points imply the connection between the mslp minimum at the preexplosive phase until the explosive phase begins.

A preferential displacement was noted in the northwest/southeast direction, indicating that the main factor of these trajectories is given by the positive/warm temperature advection (Bluestein 1993). Winter is the most dominant season, followed by spring, summer, and autumn. Spring and summer are similar concerning frequency, while autumn has the least variation.

The displacement of cyclones adheres to a natural air-mass oscillation and becomes more concentrated in lower latitudes during the year. More intense explosive cyclones transition to the north following the incursion of polar air masses during the cooler months, reaching the peak in the

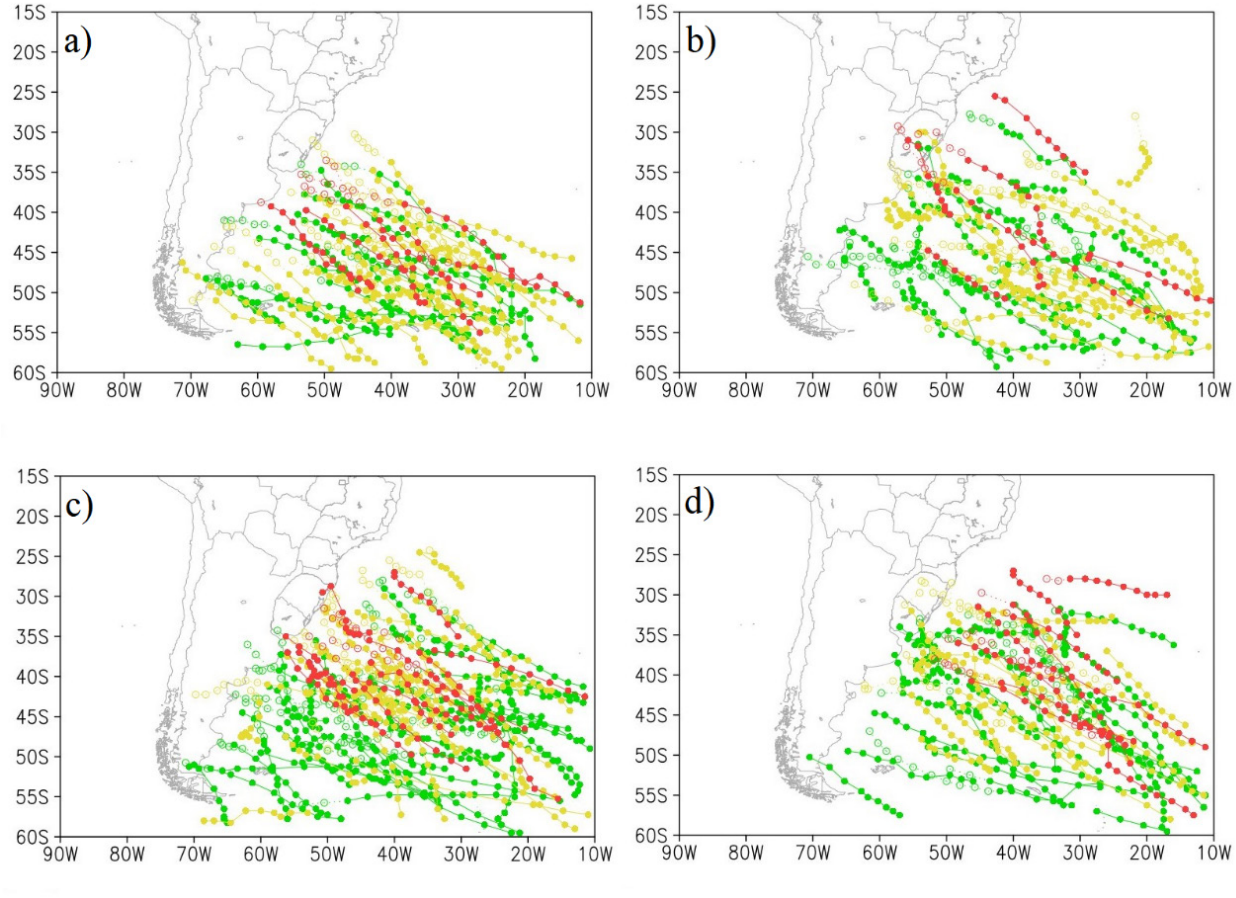

Figure 7. Explosive cyclones' trajectory (unfilled circles connected by dashed lines indicating the non-explosive phase; filled circles connected by continuous lines representing the explosive phase) distributed per season: a) summer; b) autumn; c) winter); d) spring. The green, yellow, and red trajectories are weak, moderate, and intense, respectively.

spring. This pattern reinforces what is well-known in the literature - the importance of horizontal temperature gradients as a precursor for explosive cyclones to draw energy and deepen.

Over the analyzed years, a high frequency of explosive cyclones was observed over the La Plata Region and southern Brazil, except in the summer. It is important to note that some intense cases originated in southern Brazil during autumn, possibly transitioning from the continental low. It reinforces the need to manage extreme events' impacts and mitigate life losses and socioeconomic impacts. Although the climatological region near the Gulf of San Matias shows a sign for weak explosive cyclone cases, it was not possible to point out a preferred season.

As expected, explosive cyclones are mainly oceanic events, as the abundant moisture from the ocean, supplied through the marine boundary layer processes, lowers the stability (Wang & Rogers 2001).

Automated Method (AUTM)

The method differs from others already developed. It applies to ordinary and explosive cyclones that can be studied together or separated, benefiting the study of such systems and society. In future updates, it has the potential to be applied operationally and even for climatological research and monitoring of anticyclones.

The algorithm benefits from the mslp fields, widely available in meteorological datasets. The OpenGrADS's *mfhilo* used the grid-based method, the laplacian, and the magnitude options to provide a local minimum (Murray & Simmonds 1991, Simmonds et al. 1999). In addition, the function depends on a percentile parameter, which will measure the amount of mslp minimums that will be shown. The script that runs the function is closely linked to two others coming from the shell. The latter is an environment that connects the user with the operating system and, in essence, can manipulate data. Within one of these scripts lies another important parameter: the area.

For learning purposes, the area mentioned here is equivalent to that 5° described in the OBSM (represented by the light green square in Fig. 1), except that this grid is fixed and cannot be changed according to the mslp field (role played by the black dotted frame in Fig. 1).

Sensitivity tests were applied for 2014 (highest absolute frequency by OBSM) and compared with the cases found observationally to discover the ideal percentile and area (Table II):

Table II shows the number of cyclones, only explosives, and their mean lifetimes. The 3-, 5-, 7-, and 9-degree areas were tested for the 75, 85, and 95 percentile thresholds. Unlike OBSM (ERA5 reanalysis; 3-hour temporal resolution), AUTM considered CFSR and CFSv2 and 6-hour temporal resolution. Thus, these differences were pondered in the analysis. So, we are not able to compare them but complement each other.

The research showed that the 3- and 5-degree areas are tiny to detect explosive cyclones in a 6-hour range. The 7- and 9-degree areas would be ideal for catching the most considerable variations, especially in explosive cyclones with more zonal development. These areas are the ones that most detect the explosive cyclones identified by the OBSM. However, it was chosen to be more restrictive, using 7 degrees, because the 9 degrees becomes too embracing, especially at high latitudes, where there are nearby cyclones or "parent" cyclones (they tend to dissipate or merge with the explosive cyclone).

Table II. Sensitivity tests were conducted in 2014 to find the ideal percentile and area for the dataset. The explosive cyclone cases (Nbomb); ordinary cyclone above 24 hours cases (N24H); mean ordinary cyclone lifetime (MLT24H); and mean explosive cyclone lifetime (MLTbomb) are described for each test.

Test	Percentile	Area	Nbomb	N24H	MLT24H (hours)	MLTbomb (hours)
1	75	3.0	7	193	45.0	66.6
2	75	5.0	20	294	52.8	72.6
3	75	7.0	33	342	57.0	79.8
4	75	9.0	37	356	60.6	84.6
5	85	3.0	6	118	43.8	69.0
6	85	5.0	18	205	49.2	70.2
7	85	7.0	30	245	52.8	76.2
8	85	9.0	34	256	55.2	79.8
9	95	3.0	4	55	43.8	48.0
10	95	5.0	14	119	47.4	63.0
11	95	7.0	25	151	48.6	65.4
12	95	9.0	30	159	51.0	66.6

Regarding the percentile, 75, 85, and 95 were tested (note that the percentile indicates the quantity of minimums that will be displayed in the mslp fields). It was observed that 75 ended up showing excessive points, much beyond what was seen with the OBSM. On the other hand, 85 and 95 played a significant role in detecting explosive cyclones observed by OBSM. The difference is that 95 is more restrictive and impacts the identification, reflecting in the NDR, seeing less intense explosive cyclones. With this, the 85 percentile and 7-degree area were chosen and extended from 2010 to 2020.

Bombs presented a mean lifetime greater than ordinary cyclones in 2014. The significant sample and the variety of hours that tracking can assume in these systems contribute to the results obtained. Moreover, an explosive cyclone's tracking can continue after its explosive phase until it reaches cyclolysis.

After concluding the sensitivity tests, an additional test was made to compare CFSR and ERA5 reanalyses. A 10-day sample was taken (from 00Z01012014 to 18Z01102014). The results showed that the CFSR took 2 minutes and 37 seconds while ERA5 took 30 minutes and 50 seconds. The difference is that spatial resolution from ERA5 is higher than CFSR, employing many points in a given area and leading to noisier fields. The former requires a lot of processing power and would take time to acquire the cases. Besides, the algorithm showed more than one mslp minimum for the same low pressure, leading to unreal trajectories. Even using the highest percentile, it kept illustrating the same results. Thus, we chose the CFSR and CFSv2 for the whole period.

Through sensitivity tests, Crawford et al. (2021) state that using ERA5 reanalysis at its finest resolution does not necessarily lead to better cyclone detection and tracking. The authors recommend caution when using temporal resolutions for less than 3 hours and carefully evaluating algorithm

settings. Misusing 1-hour temporal resolution breaks up the tracking into several smaller pieces. A similar process occurs when using coarse temporal resolution, such as 12 hours, resulting in late cyclogenesis identification so systems do not surpass tracking thresholds (Blender & Schubert 2000, Pinto et al. 2005, Rudeva et al. 2014).

Fig. 8 illustrates an example of the resulting plot from the *mfhilo* function. The image displays a case during July 26, 2010, with a mature cyclone near the continent and its cold front impacting Brazil's southern coast. Another mslp minimum is recorded within a surface trough near the Gulf of San Matias. Both mslp minimums are recorded in a text file and stored in folders along with their trajectories, where the shell scripts manipulate them.

During the automated method conception, many tests were made. In one of them, we noted relevant cases that surpassed the 24 hPa decaying (i.e., central pressure increasing) in a 24-hour variation. Although this analysis is beyond the scope of this research, it is interesting to know that cyclones can also exceed this rate when decaying, especially the ones that transition from high latitudes.

The advantage of this method is that a big picture of South Atlantic cyclones can be obtained, from ordinary cyclones, which have a 24-hour lifetime or more and NDR lower than 1, to explosive cyclones. This study filtered only the cases with at least a 24-hour lifetime. The analysis showed 2705 ordinary cyclones, and 299 were explosive (Table III). An average of approximately 246 ordinary and 27 explosive cyclones per year was found.

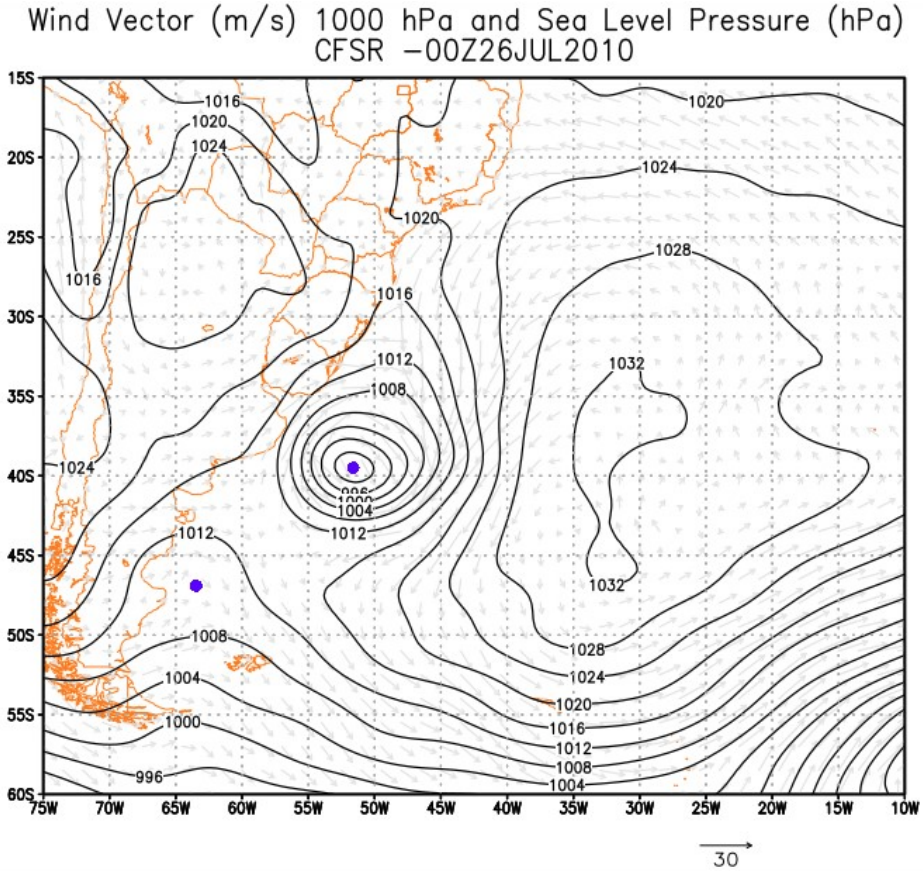

Figure 8. Example of the resulting plot for 00Z on July 26, 2010. The mslp minimums detected by the algorithm are displayed as blue dots along with the mslp field and wind field vectors in the background.

The cyclone tracks are exhibited in Fig. 9, from the red dots (cyclogenesis), through the green dots (beginning of the explosive phase) to the end of the trajectory (may encompass the non-detection of mslp minimums, the 120 hours, or domain limits). Like OBSM, cyclones can already begin as explosive; hence, the tracking will not present the red dot.

It is observed that the explosive cyclone trajectories followed, in general, what was expected from northwest to southeast. It is interesting to note the high frequency of explosive cyclones around southern Brazil. The region is known for encountering two ocean currents, becoming a site of strong

Table III. Ordinary and explosive cyclones detected by the AUTM during the studied period.

	Ordinary Cyclones	Explosive Cyclones
2010	236	22
2011	250	25
2012	263	30
2013	257	32
2014	245	30
2015	240	24
2016	237	29
2017	243	26
2018	244	32
2019	247	23
2020	243	26
Total	2705	299

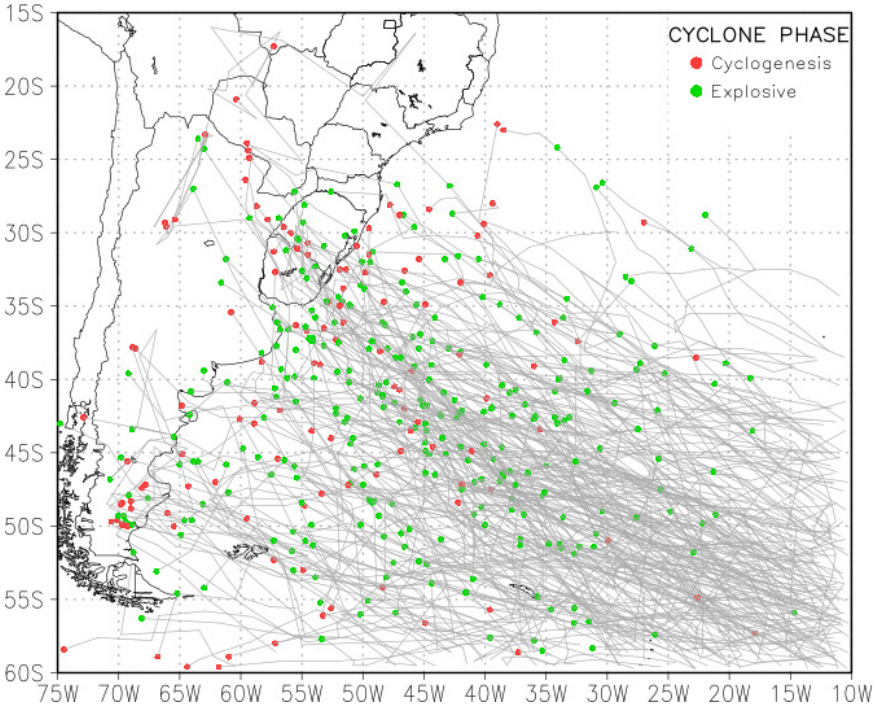

Figure 9. Explosive cyclones' trajectories identified by the automated method (AUTM) throughout the period (from 2010 to 2020). Each cyclone has its trajectory shown in gray. The red dots denote the beginning of the cyclone (cyclogenesis), and the green dots indicate the beginning of the explosive phase.

ocean and atmosphere thermal contrasts (Pezzi et al. 2005). This surface baroclinicity is one of the main forcings for explosive cyclones. In addition, the method points to the displacement of the mslp minimum transitioning from the continental low to cyclogenesis, possibly aided by the low-level jet. This last characteristic - the low-level jet parallel to the surface cold front - assists the airlifting in this region, providing convection and more robust instabilities impacting southern Brazil.

The area abovementioned and Argentina's coast, around 50°S, constitute the cyclogenetic regions of South America (Gan & Rao 1991, Reboita et al. 2010, Gramcianinov et al. 2019). As seen in Fig. 9, the latter is a cradle for cyclogenesis and explosive cyclogenesis, directly impacting the region with severe storms.

Continents are the major challenge for automated methods for cyclone detection, especially with high-resolution data. Specifically, in South America, there is an additional complication: the Andes Cordillera. Downstream the Cordillera are thermal low pressures and orographically forced lows, impacting the total statistics of explosive cyclones. Due to these systems' wide and asymmetrical shapes, variations in the mslp minimum occur in different timesteps within the 7-degree area, impacting the total statistics of explosive cyclones, especially during spring. Rudeva et al. (2014) address this problem for Tibetan Plateau and Greenland, highlighting that although orographic filtering may remove a few tracking counts, its effect on cyclone climatology is relatively localized. Also, elevated areas are essential for maintaining large-scale atmospheric dynamics, like the transition from the continental low to extratropical cyclones.

It is interesting to note the occurrence of explosive cyclones from subtropical regions. These cyclones take a hybrid form and are detected as explosives by the identification method of explosive cyclones, the NDR. The results show they occur in the autumn and spring (Fig. 10). In future approaches, it may be necessary to filter these conditions, add other identification criteria, and select only extratropical cyclones in the analysis.

Fig. 10 discretizes Fig. 9 according to the seasons. It is observed that the highest frequency is for winter (92), followed by spring (70), summer (69), and autumn (68). Seasonality showed the expected pattern, with winter peaking as the most prominent, while the other seasons show few variations in absolute frequency.

The AUTM exhibited similar behavior to the OBSM concerning the oscillation pattern, except that the former emphasizes the differences. During the summer, no intense polar masses are intaking southern Brazil (Fedorova 2001), so the most significant temperature gradients are concentrated at higher latitudes, resulting in a more zonal displacement. In the autumn, polar air masses can advance, showing the response in a slight increase in cyclogenesis, especially explosive, over southern Brazil and Uruguay's coast. However, this season still maintains a high frequency of cyclones over Argentina's coast cyclogenetic region. In winter and spring, the cyclones' trajectory displays a more prominent displacement from northwest to southeast, especially in spring, when this characteristic is more emphasized. In addition, transitioning from the continental low to explosive cyclones during spring seems to be usual according to this method – differing from MOBS (autumn). On the other hand, it is interesting to highlight the abrupt change from spring to summer, with a significant shift in the cyclone's pattern, while this aspect occurs more smoothly in other seasons.

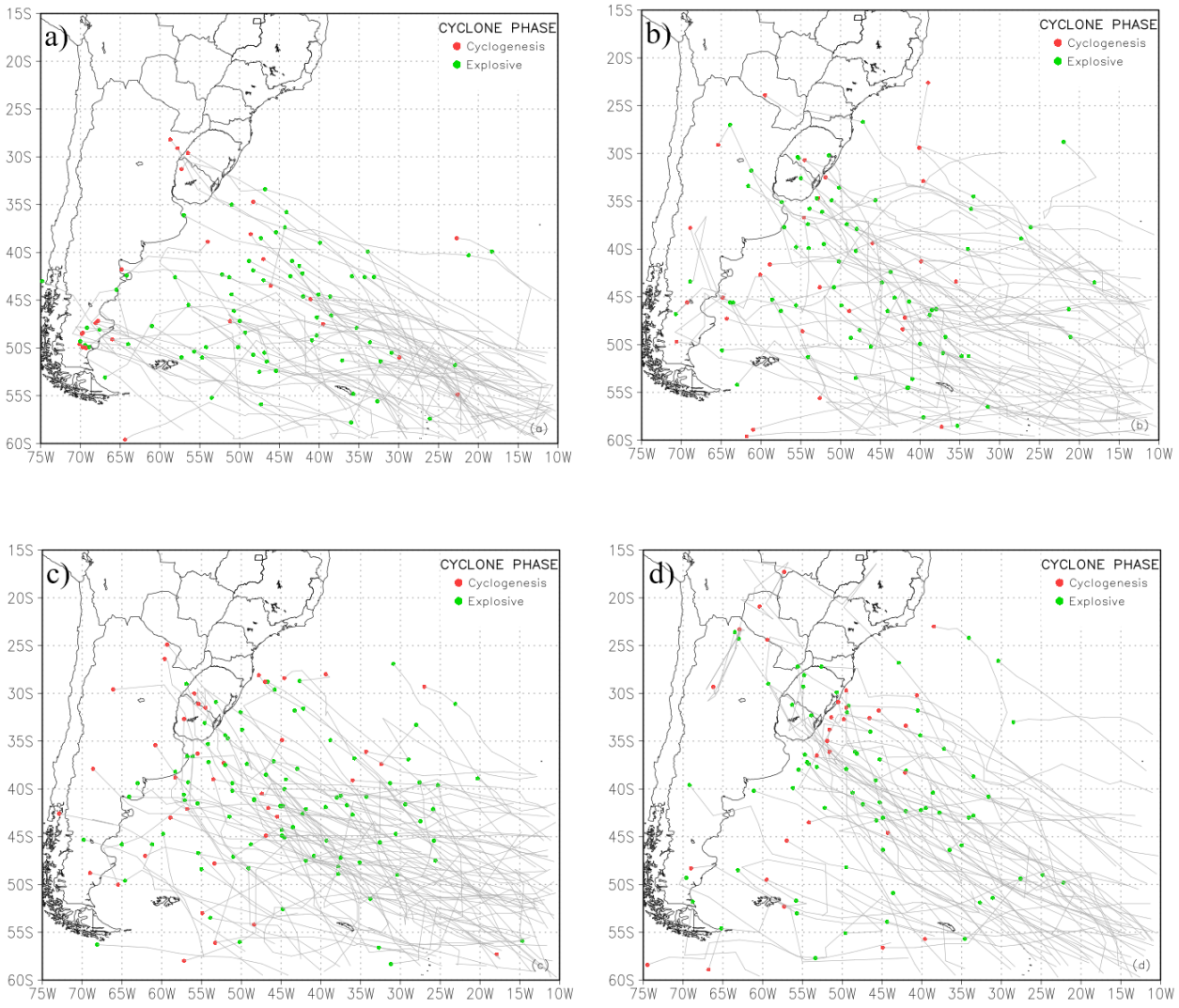

Figure 10. Explosive cyclones' trajectories detected by AUTM split into seasons: summer (top left); autumn (top right); winter (bottom left); and spring (bottom right).

CONCLUSIONS

This work aimed to contribute more to explosive cyclone studies since these systems are among the most destructive ones. For this, two detection methods were presented, one observational (OBSM) and another automated (AUTM), in an 11-year analysis (2010 to 2020) for the South Atlantic.

OBSM analysis showed that 271 cases were identified; 127 weak, 104 moderate, and 40 intense. There are 25 cases/year on average in the South Atlantic. Explosive cyclones are more frequent in winter and recurrent in June and July (especially in recent years), which agrees with the literature. It was observed that there is an oscillation over the months, in which the mean intensity increases every two months and may impact coastal regions. In addition, intense systems tend to form near Southern Brazil and Uruguay, possibly requiring baroclinicity to deepen even more. There is a trend for systems' trajectory to transition to lower latitudes over the year, following the air-masses incursion. The Gulf

of San Matias region did not present a significance seasonally, although it presents a signal for weak systems.

Regarding AUTM, sensitivity tests indicated that for CFSR and CFSv2, the best percentile is 85 with a 7-degree area. Thus, among all 2705 cyclones detected, 299 were classified as explosives. A high frequency of systems was observed over Southern Brazil, possibly aided by the low-level jet. As for the OBSM, the highest frequency was diagnosed in the winter, and the preferential displacement followed the northwest/southeast direction. In the summer, systems are confined mainly to the higher latitudes. In the autumn, there is an increase in cyclogenesis near Uruguay and Brazil's coasts. During winter and spring, the frequencies in these places mentioned above increase. Transitioning from the continental low to explosive cyclones in the spring occurred more frequently.

Each method has its advantages, and it is up to the user to choose the best way to analyze the cyclones. It is important to emphasize that comparing the methods would be unfair since they use different datasets with divergent spatial and temporal resolutions. However, these database systems obtained by OBSM serve as "truth" for validating the AUTM.

The automated method, after updates, emerges as a tool that can assist the decision-makers, being used operationally and even as a method to study the evolution of transient and semi-permanent anticyclones climatologically.

Acknowledgments

The first author would like to thank the Coordenação de Aperfeiçoamento de Pessoal de Nível Superior (CAPES) for the scholarship granted and the Federal University of Rio Grande do Sul (UFRGS), Federal Institute of Santa Catarina (IFSC), and Federal University of Pelotas (UFPel) for providing the physical spaces to conduct this research.

REFERENCES

ALLEN JT, PEZZA AB & BLACK MT. 2010. Explosive cyclogenesis: A Global Climatology Comparing Multiple Reanalyses. J Clim 23: 6468-6484.

ANDRADE HN, NUNES AB & TEIXEIRA MS. 2022. South Atlantic Explosive Cyclones in 2014-2015: Study Employing NCEP2 and MERRA-2 Reanalyses. An Acad Bras Cienc 94: e20200797. https://doi.org/10.1590/0001-3765202220200797.

AVILA VD, NUNES AB & ALVES RCM. 2021. Comparing Explosive Cyclogenesis of Different Intensities Occurred in Southern Atlantic. An Acad Bras Cienc 93: e20190157. https://doi.org/10.1590/0001-3765202120190157

BITENCOURT DP, FUENTES MV & CARDOSO CS. 2013. Climatology of explosive cyclones over cyclogenetic area of South America. Rev Bras Meteorol 28: 43-56.

BLENDER R & SCHUBERT M. 2000. Cyclone Tracking in Different Spatial and Temporal Resolutions. Mon Weather Rev 128: 377-384.

BLUESTEIN H. 1993. Synoptic-dynamic meteorology in midlatitudes. Volume II: Observations and theory of weather systems. New York: Oxford University Press, 594 p.

CRAWFORD AD, SCHREIBER EAP, SOMMER N, SERREZE MC, STROEVE J & BARBER DG. 2021. Sensitivity of Northern Hemisphere Cyclone Detection and Tracking Results to Fine Spatial and Temporal Resolution Using ERA5. Mon Weather Rev 149: 2581-2598.

DEE DP ET AL. 2011. The ERA-Interim Reanalysis: Configuration and Performance of the Data Assimilation System. Q J R Meteorol Soc 137: 553-597.

DOTY B & KINTER III JL. 1995. Geophysical Data Analysis and Visualization Using GrADS. In: Szuszczewicz EP & Bredekamp H (Eds), Visualization Techniques in Space and Atmospheric Sciences, NASA, Washington.

FEDOROVA N. 2001. Meteorologia Sinótica: Volume 2. Universidade Federal de Pelotas: Editora e Gráfica Universitária, 242 p.

FLAOUNAS E, KOTRONI V, LAGOUVARDOS K & FLAOUNAS I. 2014. "CycloTRACK (V1.0) - Tracking Winter Extratropical Cyclones Based on Relative Vorticity: Sensitivity to Data Filtering and Other Relevant Parameters. Geosc Model Dev 4: 1841-1853.

GAN MA & RAO VB. 1991. Surface Cyclogenesis over South America. Mon Weather Rev 119: 1293-1302.

GAN MA & SELUCHI ME. 2009. Ciclones e Ciclogêneses. In: Cavalcanti IFA, Dias MAF, Gertrudes M, Justi A & Ferreira NJ (Eds), Tempo e Clima no Brasil. Oficina de Textos, São Paulo, p. 111-125.

GRAMCIANINOV CB, HODGES KI & CAMARGO R. 2019. The Properties and Genesis Environments of South Atlantic Cyclones. Clim Dyn 53: 4115-4140.

GYAKUM JR, ANDERSON JR, GRUMM RH & GRUNER EL. 1989. North Pacific Cold-Season Surface Cyclone Activity: 1975-1983. Mon Weather Rev 117: 1141-1155.

HANLEY J & CABALLERO R. 2012. Objective Identification and Tracking of Multicentre Cyclones in the ERA-Interim Reanalysis Dataset, Q J R Meteorol Soc 138: 612-625.

HERSBACH H ET AL. 2020. The ERA5 Global Reanalysis. Q J R Meteorol Soc 146: 1999-2049.

HOSKINS BJ & HODGES KI. 2005. A New Perspective on Southern Hemisphere Storm Tracks. J Clim 18: 4108-4129.

LIBERATO MLR, PINTO JG, TRIGO IF & TRIGO RM. 2011. Klaus – an exceptional winter storm over northern Iberia and southern France. Weather 66: 330-334. https: //doi.org/10.1002/wea.755

LIM EP & SIMMONDS I. 2002. Explosive cyclone development in the Southern Hemisphere and a comparison with Northern Hemisphere events. Mon Weather Rev 130: 2188-2209.

LU C. 2017. A modified algorithm for identifying and tracking extratropical cyclones. Adv Atmos Sci 34: 909-924.

MENDES D, SOUZA EP, MARENGO JA & MENDES MCD. 2010. Climatology of extratropical cyclones over the South American-southern oceans sector. Theor Appl Climatol 100: 239-250.

MURRAY RJ & SIMMONDS I. 1991. A numerical scheme for tracking cyclone centres from digital data. Part I: Development and operation of the scheme. Aust Meteorol Mag 39: 155-166.

NEU U, AKPEROV MG & BELLENBAUM N. 2013. IMILAST: A community effort to intercompare extratropical cyclone detection and tracking algorithms. Bull Am Meteorol Soc 94: 529-547.

PALMÉN E & NEWTON CW. 1969. Atmospheric Circulation Systems: Their Structure and Physical Interpretation, Academic Press, New York.

PEIXOTO JP & OORT A. 1992. Physics of Climate. American Institute of Physics, New York, 520 p.

PEREIRA HR, REBOITA MS & AMBRIZZI T. 2017. Characteristics of the Atmosphere in the Austral Spring During the El Niño 2015/2016. Rev Bras Meteorol 32: 293-310.

PEZZI LP, SOUZA RB, DOURADO MS, GARCIA CAE, MATA MM & SILVA-DIAS, MAF. 2005. Ocean-atmosphere in situ observations at the Brazil-Malvinas Confluence region. Geophys Res Lett 32: L22603.

PINTO JG, SPANGEHL T, ULBRICH U & SPETH P. 2005. Sensitivities of a cyclone detection and tracking algorithm: individual tracks and climatology. Meteorol Z 14: 823-838.

PRANTL M, ZÁK M & PRANTL D. 2021. Algorithm for detecting cyclone and anticyclone centers from mean sea level pressure layer. Geosci Model Dev Discuss [preprint]. https://doi.org/10.5194/gmd-2021-266.

REALE M, LIBERATO, MLR, LIONELLO P, PINTO, JG, SALON S & ULBRICH S. 2019. A global climatology of explosive cyclones using a multi-tracking approach. Tellus A: Dyn Meteorol Oceanogr 71: 1-19.

REALE M & LIONELLO P. 2013. Synoptic climatology of winter intense precipitation events along the Mediterranean coast. Nat Hazards Earth Syst Sci 13: 1707-1722.

REBOITA MS, CRESPO NM, TORRES JA, REALE M, ROCHA RP, GIORGI F & COPPOLA E. 2021. Future Changes in winter explosive cyclones over the Southern Hemisphere domains from the CORDEX-CORE ensemble. Clim Dyn 57: 3303-3322.

REBOITA MS, ROCHA, RP, AMBRIZZI T & SUGUHARA S. 2010. South Atlantic Ocean cyclogenesis climatology simulated by regional climate model (RegCM3). Clim Dyn 35: 1331-1347.

ROEBBER PJ. 1984. Statistical Analysis and Updated Climatology of Explosive Cyclones. Mon Weather Rev 112: 1577-1589.

ROEBBER PJ, GRISE KM & GYAKUM JR. 2023. The Histories of Well-documented Maritime Cyclones as Portrayed by an Automated Tracking Method. Mon Weather Rev Early Online Release: 1-50.

RUDEVA I & GULEV SK. 2007. Climatology of Cyclone Size Characteristics and Their Changes during the Cyclone Life Cycle. Mon Weather Rev 139: 1419-1446.

RUDEVA I, GULEV SK, SIMMONDS I & TILININA N. 2014. The sensitivity of characteristics of cyclone activity to identification procedures in tracking algorithms. Tellus A: Dyn Meteorol Oceanogr 66: 24961.

SAHA S ET AL. 2006. The NCEP Climate Forecast System. J Clim 19: 3483-3517.

SAHA S ET AL. 2014. The NCEP Climate Forecast System Version 2. J Clim 27: 2185-2208.

SANDERS F. 1986. Explosive Cyclogenesis in the West-Central North Atlantic Ocean, 1981- 84. Part I: Composite Structure and Mean Behavior. Mon Weather Rev 114: 1781-1794.

SANDERS F & GYAKUM JR. 1980. Synoptic-Dynamic Climatology of the "Bomb". Mon Weather Rev 108: 1589-1606.

SATYAMURTY P, NOBRE CA & SILVA DIAS PL. 1998. South America, In: Karoly DJ & Vicent DG (Eds), Meteorology of the Southern Hemisphere, Meteorological Monographs, American Meteorological Society, p. 119-139.

SIMMONDS I, MURRAY RJ & LEIGHTON RM. 1999. A Refinement of Cyclone Tracking Methods with Data from FROST. Aust Meteorol Mag Special Issue: 35-49.

SINCLAIR MR. 1995. A climatology of Cyclogenesis for the Southern Hemisphere, Mon Weather Rev 123: 1601-1619.

SINCLAIR MR. 1997. Objective Identification of Cyclones and Their Circulation Intensity, and Climatology, Weather Forecast 12: 595-612.

WALLACE J & HOBBS P. 2006. Atmospheric Science – An Introductory Survey. Elsevier, San Diego, 486 p.

WANG CC & ROGERS JC. 2001. A Composite Study of Explosive Cyclogenesis in Different Sectors of the North Atlantic. Part I: Cyclone Structure and Evolution. Mon Weather Rev 129: 1481-1499.

WANG P, WANG P, WANG C, YUAN Y & WANG D. 2020. A Center Location Algorithm for Tropical Cyclone in Satellite Infrared Images. IEEE J Sel Top Appl Earth Obs Remote Sens 13: 2161-2172.

ZHANG S, FU G, LU C & LIU J. 2017. Characteristics of Explosive Cyclones over the Northern Pacific. J Appl Meteorol Climatol 56: 3187-3210.

How to cite

ANDRADE HN, QUADRO MFL, NUNES AB, OLIVEIRA FSC, AVILA VD, TEIXEIRA MS & ALVES RCM. 2024. Explosive cyclones occurred between 2010 and 2020 in the South Atlantic under the perspective of two detection schemes. An Acad Bras Cienc 96: e20231051. DOI 10.1590/0001-3765202420231051.

Manuscript received on September 18, 2023; accepted for publication on May 13, 2024

HUGO N. ANDRADE[1]
https://orcid.org/0000-0002-0698-2100

MÁRIO FRANCISCO L. DE QUADRO[2]
https://orcid.org/0000-0002-5904-5890

ANDRÉ B. NUNES[3]
https://orcid.org/0000-0002-4881-5810

FABRÍCIO S.C. DE OLIVEIRA[1]
https://orcid.org/0000-0002-9997-4926

VILSON D. DE AVILA[3]
https://orcid.org/0000-0001-5998-1155

MATEUS S. TEIXEIRA[3]
https://orcid.org/0000-0001-5712-9938

RITA DE CÁSSIA M. ALVES[4]
https://orcid.org/0000-0001-7804-8141

[1]Universidade Federal do Rio Grande, Instituto de Oceanografia, Avenida Itália, Km 8, 96203-900 Rio Grande, RS, Brazil

[2]Instituto Federal de Santa Catarina, Mestrado em Clima e Ambiente, Avenida Mauro Ramos, 950, 88020-300 Florianópolis, SC, Brazil

[3]Universidade Federal de Pelotas, Faculdade de Meteorologia, Campus Universitário, s/n, 96010-610 Capão do Leão, RS, Brazil

[4]Universidade Federal do Rio Grande do Sul, Centro de Pesquisas em Sensoriamento Remoto e Meteorologia, Avenida Bento Gonçalves, 9500, 91501-970 Porto Alegre, RS, Brazil

Correspondence to: **Hugo Nunes Andrade**
E-mail: hugonandrade@hotmail.com

Author contributions

Hugo Nunes Andrade, Mário Francisco Leal de Quadro, and André Becker Nunes designed the methods and analyzed the initial results. Fabrício Sanguinetti Cruz de Oliveira, Vilson Dias de Avila, and Mateus Silva Teixeira significantly contributed to the method and analysis. Rita de Cássia Marques Alves supervised the work. Hugo Nunes Andrade wrote the first draft and all authors commented on previous versions. The authors read and approved the final manuscript.